PROCEEDINGS OF SCIENCE

Overview of the Higgs boson property studies at the LHC

Giada Mancini[*, a], **Roberto Covarelli**[b †]

[a] *LNF-INFN and University of Roma Tor Vergata,* [b] *INFN and University of Torino*

E-mail: giada.mancini@lnf.infn.it, roberto.covarelli@unito.it

ATLAS and CMS results on the Standard-Model Higgs boson properties are presented. The measurements performed using the full dataset collected during Run1 (~ 5 fb^{-1} at 7 TeV and ~ 20 fb^{-1} at 8 TeV) have been presented. Newer results obtained with Run2 data (up to 3.2 fb^{-1}) collected at the center of mass energy of 13 TeV will be presented.

VII Workshop italiano sulla fisica pp a LHC
16-18 Maggio 2016
Pisa, Italy

[*] Speaker.

[†] On behalf of the ATLAS and CMS collaborations

PoS(PP@LHC2016)012

1. Introduction

The ATLAS and CMS Collaborations published the discovery of a new resonance in the search for the Standard Model (SM) Higgs boson in 2012; after that, studies have been carried out to compare its properties with the SM predictions for the Higgs boson.
The two detectors have been designed to precisely reconstruct charged leptons, photons, hadronic jets, and the imbalance of momentum transverse to the direction of the beams; they are based on different technologies requiring different reconstruction and calibration methods which reflects in different sources of systematic uncertainty.

2. State of the art after Run1

Combined ATLAS and CMS measurements of the Higgs boson production and decay rates, as well as constraints on its couplings to vector bosons and fermions have been performed during Run1 [1]. The Higgs boson production and decay rates measured by the two experiments are combined in the context of generic parameterizations based on ratios of coupling modifiers taking as input cross sections and branching fractions. The combination of the results is based on the analysis of five production processes, namely gluon fusion (ggF), vector boson fusion (VBF), and associated production with a W or a Z boson (WH, ZH) or a pair of top quarks ($t\bar{t}H$), and of the six decay modes $H \to ZZ, WW, \gamma\gamma, \tau\tau, bb$ and $\mu\mu$.
The analysis uses the CERN LHC proton-proton collision data recorded by the ATLAS and CMS experiments in 2011 and 2012, corresponding to integrated luminosities per experiment of ~ 5 fb^{-1} at 7 TeV and ~ 20 fb^{-1} at 8 TeV (Run1).

2.1 Higgs boson mass measurements

The Higgs boson mass measurement has been performed by both experiments in two of the most sensitive channels, $H \to ZZ^* \to 4\ell$ and $H \to \gamma\gamma$ which have a typical mass resolution of $1-2\%$ [2].
The results are obtained from a simultaneous fit in the two channels and for the two experiments to obtain the combined measurement of the Higgs boson mass: $m_H = 125.09 \pm 0.21(\text{stat.}) \pm 0.11(\text{syst.})$ GeV (Figure 1). The total uncertainty is dominated by the statistical term; the systematic uncertainties are dominated by effects related to the photon, electron, and muon energy or momentum scales and resolutions.
The measured masses from the individual channels and the two experiments are found to be consistent among themselves, therefore SM expectations for all the quantities entering the combined measurement in the two experiments are calculated at this mass value.

2.2 Parametrization of the signal in terms of coupling to the SM particles

2.2.1 Signal strength

The signal strength parameter (μ) is defined for an observable as the ratio between the measured Higgs boson rate and its SM expectation. The meaning of μ can vary depending on the

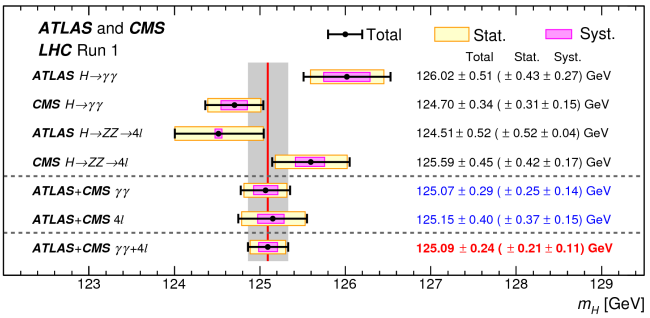

Figure 1: Measured values of the Higgs boson mass for the separated ATLAS and CMS $H \to ZZ^* \to 4\ell$ and $H \to \gamma\gamma$ channels, as well as for the combined fit in each channel and altogether.

assumptions made in each analysis; it can be defined for specific production and decay channels (as shown in Figure 2):

$$\mu_i = \frac{\sigma_i}{(\sigma_i)_{SM}} \quad \mu^f = \frac{BR^f}{(BR^f)_{SM}} \tag{2.1}$$

where σ_i is the cross section for each production mode ($i = ggF, VBF, WH, ZH, t\bar{t}H$) and BR^f is the branching ratio (BR) per final state ($f = ZZ, WW, \gamma\gamma, \tau\tau, bb$).
Due to the fact that σ_i and BR^f cannot be separately measured without additional assumptions, only the product of μ_i and μ^f can be extracted experimentally. An example of such additional assumption is that μ are the same for all production modes involving interaction with fermions (entering in the VBF and VH production modes) and with bosons (entering in the ggH and $t\bar{t}H$production mechanisms), as shown in Figure 3.

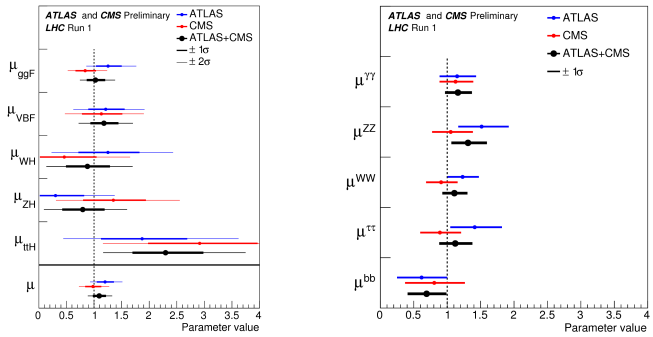

Figure 2: Results for the production (left) and decay (right) signal strengths from the combination of ATLAS and CMS. The results for each experiment are superimposed. The error bars indicate the 1σ (thick lines) and 2σ (thin lines) intervals.

2.2.2 κ-framework

The κ-framework is a formalism that has been widely used in the ATLAS and CMS Higgs boson property studies and consists in computing the $\sigma \cdot BR$ quantities by scaling the couplings of the Higgs boson to other SM particles with free parameters $\kappa = g/g_{SM}$. The coupling modifiers basically allow to parametrize specific interactions of the Higgs boson related to new physics beyond

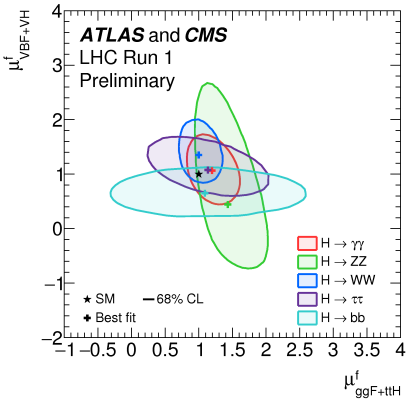

Figure 3: Likelihood contours in the ($\mu_{ggH,t\bar{t}H}$, $\mu_{VBF,VH}$) plane for the combination of ATLAS and CMS, shown for the five decay channels: $H \to ZZ, WW, \gamma\gamma, \tau\tau, bb$. The results are shown as 68% CL contours, together with the most probable values of the data and the SM expectation.

the SM effects within a leading-order motivated framework. Relying on the assumptions of the Higgs being a CP-even scalar particle and under the narrow-width approximation, the production and decay rates of the Higgs boson can be factorized, such that the $\sigma \times BR$ can be parameterized as:

$$\sigma_i \times BR^f = \frac{\sigma_i(\vec{\kappa}) \times \Gamma^f(\vec{\kappa})}{\Gamma_H} \tag{2.2}$$

where Γ_H is the total width of the Higgs boson and Γ^f is the partial width of the Higgs boson decay to the final state f. A global fit with κ parameters free for all SM particles has limited sensitivity for some of them, like κ_t and κ_b. Scenarios with more restrictive constraints dedicated to specific classes of BSM theories have also been considered, like common scale factors for all fermions and bosons defined as κ_F and κ_V (Figure 4) and no deviations have been observed with respect to the SM expectations.

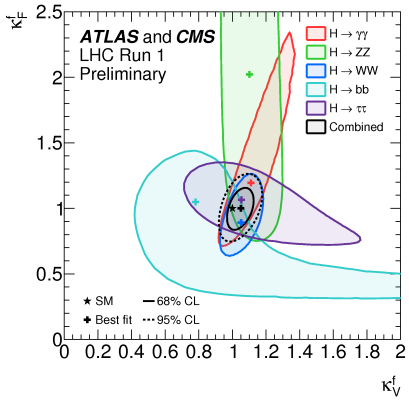

Figure 4: Confidence regions in the (κ_F, κ_V) plane for the combination of ATLAS and CMS and for the individual decay channels, assuming that all coupling modifiers are positive.

2.3 Cross sections

2.3.1 Fiducial Cross Sections

Fiducial cross sections are quoted to minimize the model dependence of the acceptance corrections related to the extrapolation to phase-space regions not covered by the detector and are corrected for detector effects to be directly compared to theoretical calculations.
In the $H \to ZZ^* \to 4\ell$ decay channel, the extraction of the signal yield for the measurement of the fiducial cross section is performed through a fit to the m_{4l} distribution using shape templates for the signal and background contributions.
The inclusive fiducial cross section measured by ATLAS [3] and CMS [4] compared to their theoretical expectations are reported below:

$$\sigma_{fid,ATLAS} = 2.11^{+0.53}_{-0.47}(\text{stat.}) \pm 0.08(\text{syst.}) \text{ fb} \quad \sigma^{SM}_{fid,ATLAS} = 1.30 \pm 0.13 \text{ fb} \tag{2.3}$$

$$\sigma_{fid,CMS} = 1.11^{+0.41}_{-0.35}(\text{stat.})^{+0.14}_{-0.10}(\text{syst.})^{+0.08}_{-0.02}(\text{model}) \text{ fb} \quad \sigma^{SM}_{fid,CMS} = 1.15^{+0.12}_{-0.13}(\text{stat.}) \text{ fb} \tag{2.4}$$

The results of all measurements are compared with theoretical calculations based on NNLO QCD results and no significant deviations are observed.

2.3.2 Differential Cross Section

The differential measurements are performed in several observables related to the Higgs boson production and decay modes, chosen to be sensitive to the Higgs boson production mechanisms as well as spin/CP quantum numbers, and among all, to test perturbative QCD predictions, probe the parton distribution functions of the proton and the relative rates of Higgs boson production modes. The measured differential cross sections in the $H \to ZZ^* \to 4\ell$, $H \to \gamma\gamma$ [5, 6] and $H \to WW^* \to 2\ell 2\nu$ [7, 8] have been compared to selected theoretical calculations of the Standard Model expectations and no significant deviation from any of the tested predictions have been found. Figure 5 shows the transverse momentum distribution on the Higgs boson in the $ZZ \to 4l$ decay channel for both experiments.

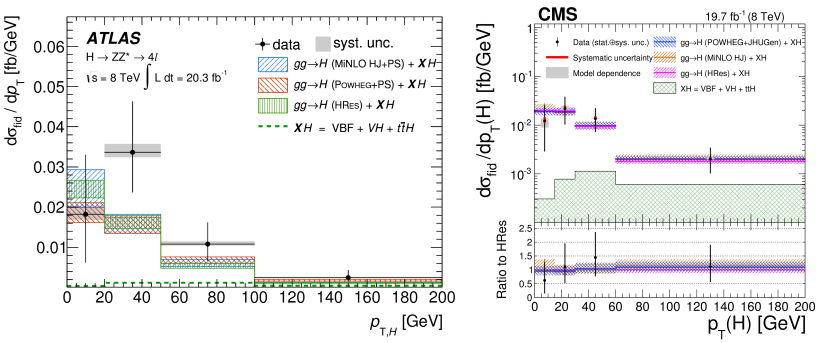

Figure 5: Results of the differential fiducial cross section measurements and comparison to the theoretical estimates for the transverse momentum of the four-lepton system in ATLAS (left) and CMS $H \to ZZ^* \to 4\ell$ (right). Theoretical estimates are superimposed, in which the acceptance of the dominant ggH contribution is modelled by several MC generators as shown in the legends.

2.4 Spin measurements

Tests on several alternatives hypothesis of spin-parity have been carried out to assert the Higgs boson as a CP-even scalar particle. Studies have been performed based on the statistical test ($\tilde{q}$) defined as the ratio of the profiled Likelihood for the data under the SM hypothesis ($J^P_{SM} = 0^+$) over the alternative hypothesis (J^P_{alt}).
Alternative hypothesis are largely disfavored by both ATLAS and CMS [9, 10] with a confidence level $> 99.9\%$. Measurements combining the channels $H \to ZZ^* \to 4\ell$, $H \to \gamma\gamma$ and $H \to WW^* \to 2\ell 2\nu$ have been also performed [11].

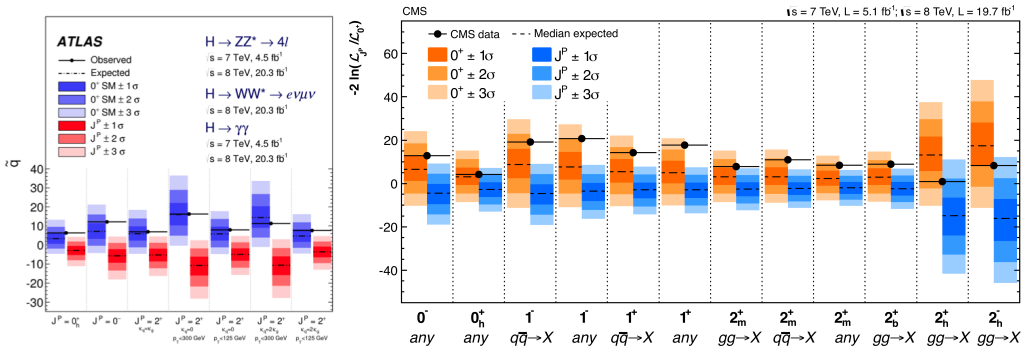

Figure 6: Summary of the expected and observed values for the test-statistic ($\tilde{q}$) distributions for the alternative hypothesis tested with respect to the SM Higgs boson in ATLAS (left) and CMS (right). The bands represents the 1, 2, and 3σ around the median expected value for the SM Higgs boson and alternative hypothesis. The black point represents the observed value.

2.5 Higgs width

Despite the experimental resolution being orders of magnitude greater than what would be needed to directly measure the Higgs boson width, constraints on its width can be obtained measuring the off-shell Higgs boson event yields normalized to the Standard Model prediction (μ) in the $ZZ \to 4l$, $ZZ \to 2l2\nu$ and $WW \to e\nu\mu\nu$ final states following the relation given by:

$$\frac{\mu^{off-shell}}{\mu^{on-shell}} = \frac{\Gamma_H}{\Gamma_H^{SM}} \tag{2.5}$$

Observed upper limit on the Higgs boson width have been set [12, 13] with a confidence level (CL) of 95%, namely:

$$\frac{\Gamma_H}{\Gamma_H^{SM}} < 4.8 - 7.7(7.0 - 12) \quad \text{given for } 0.5 < R^B_{H^*} < 2.0 \quad \text{(ATLAS)} \tag{2.6}$$

$$\frac{\Gamma_H}{\Gamma_H^{SM}} < 3.2(6.5) \quad \text{(CMS)} \tag{2.7}$$

where numbers in parenthesis are the corresponding expected upper limit and $R^B_{H^*}$ is the ratio of the gg-induced background over the signal in the off-peak region ($R^B_{H^*} = \frac{k(gg\to ZZ)}{k(gg\to H^*\to ZZ)}$), which is not precisely known from theory. The range $0.5-2$ is chosen for the variation of the k-factor ratio $R^B_{H^*}$ in order to include the full correction from the signal k-factor $k(gg \to H^* \to ZZ)$ in the variation range.

3. First results from Run2

3.1 $H \to ZZ^* \to 4\ell$

The event selection in the $H \to ZZ^* \to 4\ell$ decay cannel is characterized by the selection of high-quality leptons, including final-state-radiation recovery, with high efficiency; the background estimate is based on Monte Carlo (MC) simulations for the $ZZ^{(*)}$ and from control region in data for the so-called reducible backgrounds (mainly $Z+X$). The signal extraction in ATLAS [14] is performed via a fit to the $m_{4\ell}$ distribution after a kinematic fit with a constrained Z mass while in CMS [16] two signal categories are defined (VBF-tagged events and other events) and the bare $m_{4\ell}$ plus a matrix-element-based kinematic discriminant are used to perform the analysis. Of course the results are limited by the very small statistics recorded. Figure 7 (right) shows the $m_{4\ell}$ distribution observed by CMS with the early 13 TeV dataset.
The global signal strength measured by CMS is $\mu^{4l} = 0.89^{+0.62}_{-0.46}$ with the fiducial cross section being $\sigma^{4l}_{\text{fid.}} = 2.48\ ^{+1.48}_{-1.14\,\text{stat+syst.}}\ ^{+0.01}_{-0.04\,\text{model dep.}}$ fb, in very good agreement with the SM expectation.

3.2 $H \to \gamma\gamma$

The key points of the $H \to \gamma\gamma$ decay channel are the very good energy resolution and photon selection. The ATLAS analysis [17] uses a cut-based approach for this selection, while CMS [18] uses a multivariate approach and various signal categories for a measurement of the signal strength in different production modes.
The variables used are based on the shape and the expected containment of the showers, track and calorimeter isolation, and the rejection of π^0 decays. Another important aspect of the di-photon mass reconstruction is the identification of the primary vertex, where CMS adopts a multivariate analysis using the Σp_T^2 of tracks in the vertex and their balancing with respect to the di-photon system and ATLAS uses a similar technique supplemented with photon trajectory estimates from the pointing calorimeter. Both experiments fit the distribution of $m_{\gamma\gamma}$ in signal categories of different purity. Figure 7 (left) shows the inclusive distribution as observed in ATLAS 13 TeV data.

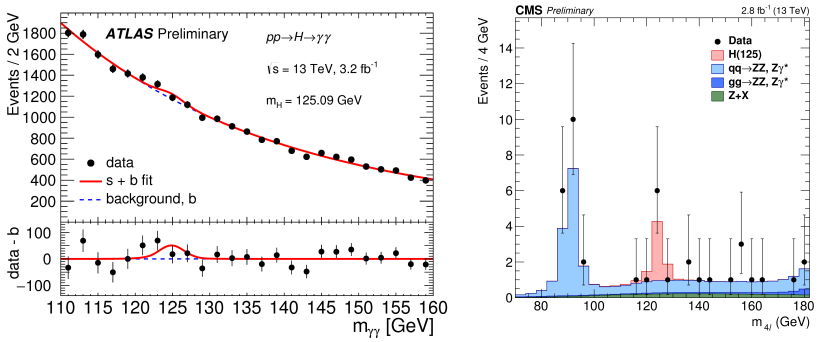

Figure 7: (left) Diphoton invariant-mass spectrum observed in the 13 TeV ATLAS data. The solid red curve shows the fitted signal plus background model when the Higgs boson mass is fixed at 125.09 GeV. The background component of the fit is shown with the dotted blue curve. The bottom plot shows the residual of the background-subtracted data. (Right) Distribution of the four-lepton invariant mass observed in the 13 TeV CMS data.

The global signal strength measured by CMS for this signal is $\mu^{\gamma\gamma} = \sigma/\sigma_{SM} = 0.69^{+0.47}_{-0.42}$ fully compatible with SM expectation; from ATLAS instead we have a measurement of the fiducial cross section: $\sigma^{\gamma\gamma}_{\text{fid.}} = 52 \pm 34_{\text{stat.}}\,^{+21}_{-13\,\text{syst.}} \pm 3_{\text{lumi.}}$ fb.

4. Conclusion

The Run1 LHC data taking has been characterized by the Higgs boson discovery with a mass of $m_H = 125.09 \pm 0.21(\text{stat.}) \pm 0.11(\text{syst.})$ GeV with evidence in the gluon fusion and vector-boson fusion production modes.
After the Higgs boson discovery, measurements of its properties have been performed to assure the consistency of the couplings of the Higgs with the SM expectations: among this results we can quote the combined signal strength found to be perfectly consistent with the SM predictions: $\mu = 1.09 \pm 0.07(\text{stat.}) \pm 0.04(\text{exp.syst.}) \pm 0.03(\text{th.bkg.})^{+0.07}_{-0.06}(\text{th.sig})$.
Tests for different spin-parity hypothesis exclude non SM J^P hypothesis with $CLs > 99.9\%$ and indirect limits on the Higgs boson width quote results better than $\Gamma_H < 5 \times \Gamma_H^{SM}$ at 95% CL.
The first Run2 data have been very useful in order to optimize the analyses in view of a precise measurement of the Higgs boson properties. More data will allow high precision measurements in the near future.

References

[1] ATLAS and CMS Collaborations: Measurements of the Higgs boson production and decay rates and constraints on its couplings from a combined ATLAS and CMS analysis of the LHC pp collision data at $\sqrt{s} = 7$ and 8 TeV (ATLAS-CONF-2015-044, CMS-PAS-HIG-15-002, arXiv:1606.02266).

[2] ATLAS and CMS Collaborations: Combined Measurement of the Higgs Boson Mass in pp Collisions at $\sqrt{s} = 7$ and 8 TeV with the ATLAS and CMS Experiments (Phys. Rev. Lett. **114** (2015) 191803).

[3] ATLAS Collaboration: Fiducial and differential cross sections of Higgs boson production measured in the four-lepton decay channel in pp collisions at $\sqrt{s} = 8$ TeV with the ATLAS detector (Phys. Lett. B **738** (2014) 234).

[4] CMS Collaboration: Measurement of differential and integrated fiducial cross sections for Higgs boson production in the four-lepton decay channel in pp collisions at $\sqrt{s} = 7$ and 8 TeV (JHEP **04** (2016) 005).

[5] ATLAS Collaboration: Measurements of fiducial and differential cross sections for Higgs boson production in the diphoton decay channel at $\sqrt{s} = 8$ TeV with ATLAS (JHEP **09** (2014) 112).

[6] CMS Collaboration: Measurement of differential cross sections for Higgs boson production in the diphoton decay channel in pp collisions at $\sqrt{s} = 8$ TeV (Eur. Phys. J. C 76 (2016) 13).

[7] ATLAS Collaboration: Measurement of fiducial differential cross sections of gluon-fusion production of Higgs bosons decaying to $WW^* \to e\nu\mu\nu$ with the ATLAS detector at $\sqrt{s} = 8$ TeV (arXiv:1604.02997).

[8] CMS Collaboration: Measurement of the transverse momentum spectrum of the Higgs boson produced in pp collisions at $\sqrt{s} = 8$ TeV using H to WW decays (arXiv:1606.01522, CMS PAS HIG-15-010).

[9] CMS Collaboration: Observation of the diphoton decay of the Higgs boson and measurement of its properties (Eur. Phys. J. C 74 (2014) 3076).

[10] CMS Collaboration: Measurement of the properties of a Higgs boson in the four-lepton final state (Phys. Rev. D (2014) **89**, 092007).

[11] ATLAS Collaboration: Study of the spin and parity of the Higgs boson in diboson decays with the ATLAS detector (Eur. Phys. J. C 75 (2015) 476).

[12] ATLAS Collaboration: Constraints on the off-shell Higgs boson signal strength in the high-mass ZZ and WW final states with the ATLAS detector (Eur. Phys. J. C 75 (2015) 335).

[13] CMS Collaboration: Search for Higgs boson off-shell production in proton-proton collisions at 7 and 8 TeV and derivation of constraints on its total decay width (arXiv:1605.02329).

[14] ATLAS Collaboration: Measurements of the Higgs boson production cross section at 7, 8 and 13 TeV centre-of-mass energies and search for new physics at 13 TeV in the $H \to ZZ^* \to l^+l^-l^{'+}l^{'-}$ final state with the ATLAS detector (ATLAS-CONF-2015-059).

[15] ATLAS Collaboration: Measurements of the total cross sections for Higgs boson production combining the $H \to \gamma\gamma$ and $H \to ZZ^\star \to 4l$ decay channels at 7, 8 and 13 TeV center-of-mass energies with the ATLAS detector (ATLAS-CONF-2015-069).

[16] CMS Collaboration: Studies of Higgs boson production in the four-lepton final state at $\sqrt{s} = 13$ TeV (CMS-PAS-HIG-15-004).

[17] ATLAS Collaboration: Measurement of the Higgs boson production cross section at 7, 8 and 13 TeV center-of-mass energies in the $H \to \gamma\gamma$ channel with the ATLAS detector (ATLAS-CONF-2015-060).

[18] CMS Collaboration: First results on Higgs to $\gamma\gamma$ at 13 TeV (CMS-PAS-HIG-15-005).